Development 129, 187-196 (2002)
Printed in Great Britain © The Company of Biologists Limited 2002
DEV5960

The stem-loop binding protein CDL-1 is required for chromosome condensation, progression of cell death and morphogenesis in *Caenorhabditis elegans*

Yuki Kodama[1], Joel H. Rothman[2], Asako Sugimoto[1,3,4,*] and Masayuki Yamamoto[1]

[1]Department of Biophysics and Biochemistry, Graduate School of Science, University of Tokyo, Bunkyo, 113-0032, Japan
[2]Neuroscience Research Institute, University of California-Santa Barbara, Santa Barbara, CA 93106, USA
[3]PRESTO, Japan Science and Technology Corporation, Kawaguchi, 332-0012, Japan
[4]Laboratory for Developmental Genomics, RIKEN Center for Developmental Biology, Kobe, 650-0047 Japan
*Author for correspondence [e-mail: sugimoto@ims.u-tokyo.ac.jp, sugimoto@cdb.riken.go.jp (from April 2002)]

Accepted 5 October 2001

SUMMARY

Histones play important roles not only in the structural changes of chromatin but also in regulating gene expression. Expression of histones is partly regulated post-transcriptionally by the stem-loop binding protein (SLBP)/hairpin binding protein (HBP). We report the developmental function of CDL-1, the *C. elegans* homologue of SLBP/HBP. In the *C. elegans cdl-1* mutants, cell corpses resulting from programmed cell death appear later and persist much longer than those in the wild type. They also exhibit distinct morphological defects in body elongation and movement of the pharyngeal cells toward the buccal opening. The CDL-1 protein binds to the stem-loop structures in the 3′-UTR of *C. elegans* core histone mRNAs, and the mutant forms of this protein show reduced binding activities. A decrease in the amount of core histone proteins phenocopied the *cdl-1* mutant embryos, suggesting that CDL-1 contributes to the proper expression of core histone proteins. We propose that loss-of-function of *cdl-1* causes aberrant chromatin structure, which affects the cell cycle and cell death, as well as transcription of genes essential for morphogenesis.

Key words: *Caenorhabditis elegans*, Chromatin structure, Histone, SLBP, Programmed cell death, Morphogenesis, CDL-1

INTRODUCTION

Chromatin changes its structure dynamically in the processes of mitosis and apoptosis, as well as during various states of cell differentiation (reviewed by Kornberg and Lorch, 1999; Cheung et al., 2000). In mitosis, chromatin undergoes a high degree of condensation, which is essential for proper chromosome segregation. During apoptosis, chromatin condensation and nuclear pycnosis occur in concert with DNA degradation to nucleosome-length units (reviewed by Robertson et al., 2000). Chromatin structure is also an important element for regulating gene expression. Recent studies suggest that chromatin structural changes often are the result of chemical modification of histone proteins, such as phosphorylation and acetylation (reviewed by Cheung et al., 2000).

A histone octamer includes two molecules each of four types of core histones, H2A, H2B, H3 and H4. A histone octamer is assembled with ~200 bp of DNA to form a nucleosome, a repeating unit of the chromatin structure (reviewed by Kornberg and Lorch, 1999). Biosynthesis of histones is tightly regulated during the cell cycle at both transcriptional and posttranscriptional levels. The abundance of histone mRNA increases 25- to 35-fold as the cell progresses from G_1 to S phase as the result of increased transcription and stabilization of mRNA (reviewed by Osley, 1991). Transcription is induced three- to 10-fold by the NPAT-cyclin E/CDK2 pathway at the G_1/S boundary in mammalian cells (Ma et al., 2000; Zhao et al., 2000). Metazoan replication-dependent histone mRNAs do not have poly(A) tails. Instead these messages have conserved stem-loop structures in their 3′-UTRs, which are essential for posttranscriptional regulation, including, pre-mRNA processing, nuclear export, translation, and stabilization/destabilization of the mRNAs (Harris et al., 1991; Luscher and Schumperli, 1987; Mowry et al., 1989; Pandey and Marzluff, 1987; Stauber et al., 1986; Stauber and Schumperli, 1988; Sun et al., 1992).

The stem-loop binding proteins (SLBPs)/hairpin-binding proteins (HBPs) were initially cloned from mammals based on their ability to bind to the stem-loop structure of replication-dependent histone mRNAs (Martin et al., 1997; Wang et al., 1996). Biochemical studies suggested that SLBPs play major roles in the post-transcriptional regulation of core histone pre-mRNA. One of the proposed functions of SLBP is to stabilize the interaction between U7 snRNP and histone pre-mRNA, which is an essential step for 3′ end cleavage of the pre-mRNA (Dominski et al., 1999). After the processing, SLBPs remain associated with the stem-loop and accompany the mRNAs to

the cytoplasm, where they are involved in histone mRNA translation and stability (Gallie et al., 1996; Muller and Schumperli, 1997; Williams et al., 1994). Two SLBPs, namely xSLBP1 and xSLBP2, each with distinct functions, have been isolated from *Xenopus laevis* oocytes (Wang et al., 1999). While xSLBP1 is involved in 3′ end processing of histone mRNAs, xSLBP2 does not appear to be involved in this processing. The latter functions in storage of histone mRNA during oogenesis (Ingledue et al., 2000; Wang et al., 1999). More recently, the SLBP of *Drosophila melanogaster*, dSLBP, was identified and mutations in its structural gene were isolated. Genetic analyses of the gene has shown that dSLBP is essential for proper histone expression in *Drosophila* (Sullivan et al., 2001). In the nematode *Caenorhabditis elegans*, a gene was isolated that shares homology to other SLBP/HBP genes only within the RNA-binding domain (Martin et al., 1997). The product of this gene was shown to bind to the stem-loop of the histone mRNA of *C. elegans*, but not to that of humans (Michel et al., 2000). However, the in vivo function of the *C. elegans* SLBP has not been examined.

In this report, we describe mutants of the *C. elegans* SLBP gene, *cdl-1* (cell death lethal). The *cdl-1* mutants were originally identified based on their zygotic embryonic lethal phenotype, in which arrested embryos accumulate dead cells (cell corpses) and show particular morphogenetic defects. Our analyses indicate that the *C. elegans* SLBP encoded by *cdl-1* is essential for proper core histone expression in vivo, and loss of its function affects mitosis, programmed cell death and morphogenesis.

MATERIALS AND METHODS

Strains and genetic methods

Maintenance and genetic manipulation of *C. elegans* were carried out as described (Brenner, 1974). Strains used were: wild-type *C. elegans* var. Bristol, strain N2; (LGI) *ced-1(e1735)*; (LGII) *cdl-1(e2501, e2510, w37)* (this study), *mnDf83, mnDf87, mnDf89, mnDf90, dpy-10(e128), unc-104(e1265), mnC1[dpy-10(e128) unc52(e444)]*; (LGIII) *ced-4(n1162), ced-9(n1950)*; (LGIV) *ced-3(n717), ced-5(n1812)*. Strains were maintained at 20°C.

Microscopy

Microscopic images were taken using a cooled CCD camera (Hamamatsu Photonics) attached to a Zeiss Axiophot or a Zeiss Axioplan 2 microscope, and stored digitally using either NIH Image or Fish Imaging Software (Hamamatsu Photonics). 4D images were taken using the 4D grabber PPC software (kindly provided by Charles Thomas, http://www.loci.wisc.edu/4d/native/4d.html) on an Axiophot with a Microscope Focus Controller (ASI), and characterized with the 4D Viewer PPC software (provided by C. Thomas). Quantification of the number and duration of cell corpses was described elsewhere (Sugimoto et al., 2001).

Cloning of *cdl-1*

cdl-1 was genetically mapped to the right of *dpy-10* on chromosome II. Genomic deficiencies, *mnDf83*, *mnDf89* and *mnDf90* failed to complement the lethality of *e2510* and *e2501* animals, while *mnDf87* could complement. Cosmids that map in this region were introduced into either *e2510* or *e2501* heterozygotes by germline transformation (Mello and Fire, 1995), and their ability to rescue embryonic lethality was tested. For rescue of the *cdl-1* mutants, cosmids were injected at 1-10 ng/μl using the co-injection markers pRF4 [*rol-6(su1006dm)*] (Mello et al., 1991) and/or pPDEF1α (*EF1α::gfp*) (provided by Makoto Koga) at 10-40 ng/μl. The cosmid T19E10 completely rescued the embryonic lethality of *e2510* and *e2501*, and some of the rescued *cdl-1* homozygous animals grew into fertile adults. Rescue with the cosmid T19E10 was also confirmed by introducing an extrachromosomal array from the transgenic strain with *sEx731* [T19E10 (II)+pCes1943{*rol-6(su1006dm)*}] [provided by the *C. elegans* Transgenic Library Project (Janke et al., 1997)]. C52A11 and R06F6, the cosmids overlapping T19E10, did not rescue the mutants.

We performed RNA interference (RNAi) (Fire et al., 1998) for all the ORFs predicted on the cosmid T19E10, by injecting double-stranded RNA corresponding to each ORF into wild-type adult worms. Some F_1 embryos that were fertilized 5 hours after the injection of dsRNA corresponding to R06F6.1 phenocopied the *cdl-1* genomic mutants (Fig. 7B,C). Most *R06F6.1(RNAi)* embryos fertilized later than 5 hours arrested early in embryogenesis. To confirm that R06F6.1 is *cdl-1*, we identified the molecular lesion in the corresponding coding region for all three *cdl-1* alleles. We found that *e2510* carried a missense mutation whereas *e2501* carried a nonsense mutation that could result in a truncated protein. *w37* carried a 4.7kb deletion that removed the entire R06F6.1 ORF and part of the neighboring ORF (T19E10.1), with a small insertion of ~60 bp instead. These results indicate that R06F6.1 corresponds to the *cdl-1* gene.

Although *w37* deletes part of T19E10.1 in addition to *cdl-1*, the embryonic phenotype of *w37* is likely to reflect the null phenotype of the *cdl-1* gene, because deletion of T19E10.1 leads to the Stu (sterile and uncoordinated) phenotype and shows no apparent embryonic phenotype (Y. K. and A. S., unpublished observation; M. Ohmachi, E. Lambie, P. Kuwabara and T. Schedl, personal communication).

The sequence of the cDNA clone yk376d1 (provided by Y. Kohara) that corresponds to the *cdl-1* gene (=R06F6.1) was determined and deposited in GenBank (accession number AB060649). This clone apparently contains the whole protein-coding region.

RNA interference

The cDNA clones, yk376d1 and yk393d3 (provided by Y. Kohara) were used as the templates to prepare antisense and sense *cdl-1* RNA (Fire et al., 1998). A mixture of both strands was microinjected into wild-type young adult hermaphrodites. F_1 embryos from these injected worms were examined.

For the histone RNAi experiments, the cDNA clones yk213a4 (histone H3), yk245d10 (histone H4), yk261a8 (histone H2B, all provided by Y. Kohara), and H2A ORF clone were used as the templates and examined as above. As for the histone H2A clone, predicted ORF ZK131.10 (*his-16*) (Roberts et al., 1989), which encodes histone H2A carrying the conserved stem-loop in their 3′-UTR, was amplified from *C. elegans* genome using PCR, and was subcloned into pBluescript vector. To weaken the RNAi effect so that late embryonic phenotypes could be analyzed, RNA solutions synthesized with either T3 or T7 RNA polymerase alone (and therefore containing mostly single-stranded RNA) were injected.

Yeast three-hybrid system

The yeast L40-coat strain and plasmid pIII/MS2-1 (for RNA bait), and the positive controls, pIIIA/IRE-MS2, and pAD-IRP (SenGupta et al., 1996), were gifts from Marvin Wickens. The strain L40-coat carries an integrated copy of the LexA-MS2 coat protein fusion gene. The plasmids wtRNA or rvRNA were constructed by digesting plasmid pIII/MS2-1 with *Sma*I and inserting a 34-nucleotide double-stranded oligonucleotide containing either the wild-type or the reversed stem-loop sequence, respectively (see Fig. 6). To construct a GAL4 activation domain fusion protein, the plasmid pACT2, modified for Gateway Cloning Technology (Life Technologies), was used. The wild-type CDL-1 sequence was introduced from the cDNA clone yk376d1 (provided by Y. Kohara). To assay the binding ability of the mutant proteins, site-directed mutagenesis with PCR was used to incorporate the specific mutations. Each pair of these plasmids was

transformed into the yeast strain L40-coat as described in the manual povided by Clontech. The transformants were selected by plating on media minus leucine (–Leu), –Ade, –Ura, –Trp plates. The resulting colonies were tested for β-galactosidase activity by the colony-lift filter assay as described in the same manual. To examine *HIS3* expression, these colonies were tested for growth on –His, –Leu, –Ade, –Ura, –Trp plates containing 5 mM aminotriazole.

Immnofluorescence

Embryos were processed for staining as described previously (Miller and Shakes, 1995). In brief, embryos permeabilized by the freeze-crack method were fixed by placing in methanol for 5 minutes at room temperature. Rehydrated embryos were treated with blocking solution [1% skim milk 5% fetal bovine serum in PBST (phosphate-buffered saline containing 0.5% Tween-20)] for 30 minutes at room temperature and incubated with the primary antibody overnight at 4°C and then with the secondary antibody for 1-2 hours at room temperature. DAPI was added to a final concentration of 2 μg/ml, and the sample was mounted for epifluorescence microscopy.

Antibodies used were: anti-alpha tubulin antibody DM1A (SIGMA), 3NB12 [early marker for pharynx (Priess and Thomson, 1987)], FITC-conjugated sheep anti-mouse IgG antibody (ORGANON TEKNIKA), and Cy3-labeled goat anti-mouse IgG antibody (AP124C, CHEMICON).

RESULTS

Excess cell corpses accumulate in *cdl-1* embryos

In a genome-wide screen for zygotic embryonic lethal (ZEL) mutations (J. H. Rothman, unpublished), we identified three allelic recessive mutations (*e2501*, *e2510* and *w37*) that cause accumulation of excess cell corpses at the terminal arrest stage, as well as defects in body elongation and pharyngeal development (Fig. 1). We named the locus *cdl-1* (cell death lethal).

Of the 671 cells produced during embryogenesis in *C. elegans*, 113 cells undergo programmed cell death. The dead cells are engulfed by neighboring cells within ~10 minutes. Terminal *e2510*, *e2501* and *w37* embryos contained more than 8 cell corpses, compared to zero in wild-type embryos at the time of hatching. To characterize the temporal change in the number of cell corpses, the development of *cdl-1* embryos was observed over time with Nomarski microscopy and the cell corpses in each embryo were scored periodically (Fig. 2).

Wild-type embryos generate their first cell corpse at 220 minutes and hatch at around 800 minutes after first cleavage (Sulston et al., 1983). We divided the intermediate period into six stages (I to VI). In wild-type embryos most (110 out of 113) cell death occurs during stages I to III of development, corresponding to the period between 220 and 510 minutes after first cleavage (Fig. 2A). (Note that since cell corpses are normally engulfed rapidly, only a fraction of cells that have undergone programmed cell death show up as cell corpses at any one time point.) In *cdl-1* embryos, fewer corpses were observed during stages I and II (220~410 minutes) but significantly more corpses accumulated at stages IV to VI (520~810 minutes) compared to the wild type (Fig. 2B-D). At stage V (620~710 minutes), 21, 15 and 11 corpses on average were observed in the *e2510*, *e2501* and *w37* embryos respectively, in contrast to no or only one corpse seen in wild-type embryos.

CED-3, CED-4 and CED-9 constitute an evolutionarily conserved complex ‘apoptosome’ that is part of the regulatory machinery for the normal programmed cell killing process (reviewed by Metzstein et al., 1998). To confirm that the cell corpses in *cdl-1* mutants are produced by the normal programmed cell death pathway, we constructed double mutants of *cdl-1(e2510)* with either *ced-3(n717)*, *ced-4 (n1162)* or *ced-9(n1950gf)*, which suppress programmed cell death almost completely (Ellis and Horvitz, 1986; Hengartner et al., 1992). The production of cell corpses was blocked in all of the double mutants (data not shown), indicating that the cell corpses seen in *cdl-1* embryos arose by the genetically programmed cell death.

The appearance and elimination of cell corpses is delayed in *cdl-1* embryos

To characterize the cell death phenotype of *cdl-1* mutants in more detail, we recorded embryogenesis using a 4 D (4 dimensional) time-lapse apparatus and followed each cell corpse. Most cell corpses in *cdl-1(e2510)* embryos appeared much later than those in the wild type: only ~10 corpses were observed in *e2510* embryos between 220 and 470 minutes after first cleavage, during which wild-type embryos generated most cell corpses (Fig. 3A,B). Furthermore, while the majority of cell corpses in wild-type embryos disappeared within ~20 minutes, most corpses persisted much longer in *cdl-1(e2510)* embryos, as long as several hours (Fig. 3B). Thus, mutations in *cdl-1* lead to delayed appearance and persistent presence of cell corpses. This is unlikely to be caused by a general delay in embryogenesis, since the rate of cell division was not significantly affected in *cdl-1(e2510)* embryos, at least in some lineage of the AB decendant (data not shown). Therefore, *cdl-1* appears to be required for the timely generation and elimination of cell corpses.

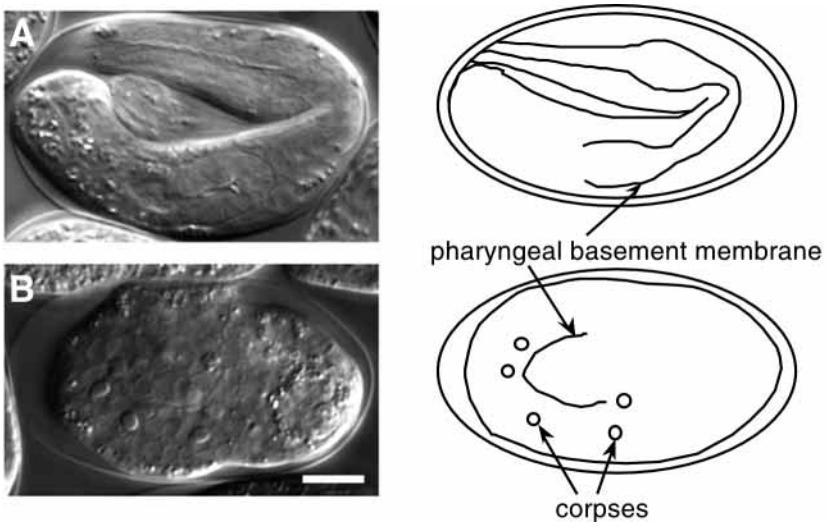

Fig. 1. *cdl-1* gross phenotypes. A wild-type N2 embryo at the pretzel stage (A) and a *cdl-1(e2510)* embryo (B) are shown. Terminally arrested *cdl-1* embryos show excess cell corpses, variable defects in body elongation, and a failure in attachment of the pharynx to the buccal opening. Scale bar, 10 μm.

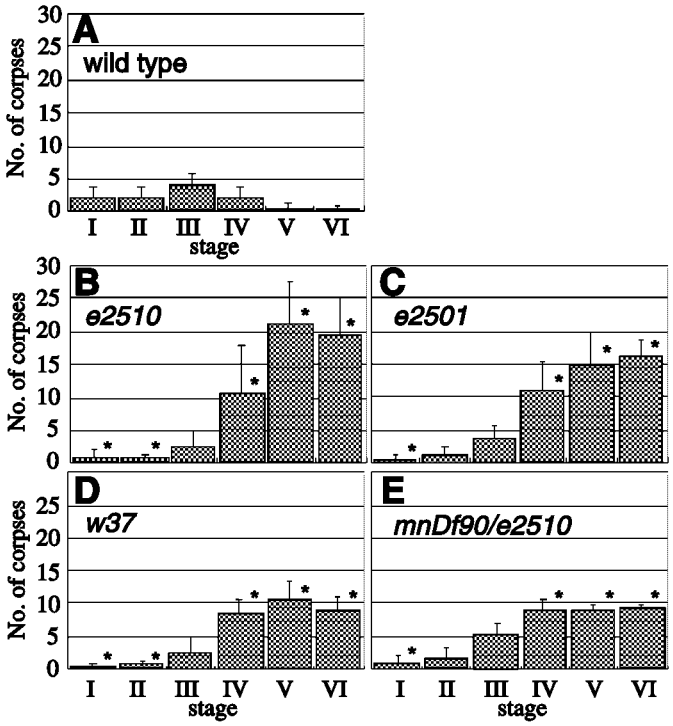

Fig. 2. Quantitation of the number of cell corpses during embryogenesis. (A) Wild-type N2. (B) *cdl-1(e2510)*. (C) *cdl-1(e2501)*. (D) *cdl-1(w37)*. (E) *mnDf90/cdl-1(e2510)*. The y axis represents the average number of cell corpses visible in embryos of each genotype at each stage. Stages are defined as follows: 220~310 minutes (I), 320~410 minutes (II), 420~510 minutes (III), 520~610 minutes (IV), 620~710 minutes (V), and 720~810 minutes (VI) after first cleavage. Error bars indicate s.d. Numbers of embryos examined were (A) 17, (B) 23, (C) 11, (D) 8 and (E) 32, respectively. Asterisks (*) indicate that the difference from the wild type at the same stage is significant (P<0.01).

To determine whether *cdl-1* is involved in the cell corpse engulfment pathways previously identified, we tested for genetic interaction of *cdl-1* with known engulfment-associated genes. Known genes involved in engulfment have been divided into two genetically distinct groups, represented by *ced-1* and *ced-5* respectively (Ellis et al., 1991). In both *ced-1(e1735); cdl-1(e2510)* and *ced-5(n1812); cdl-1(e2510)* embryos, the number of cell corpses was significantly increased compared with each single mutant (data not shown). Thus, *cdl-1* is unlikely to belong to either of the two known engulfment pathways.

cdl-1 embryos are defective in body elongation and pharyngeal extension

Wild-type embryos undergo dramatic elongation starting at ~350 minutes after first cleavage (Sulston et al., 1983). Body elongation proceeds as hypodermal cells change their shapes, elongating longitudinally in concert with circumferential contraction (Priess and Hirsh, 1986). All *cdl-1* alleles showed some defect in body elongation, though with some variability. Most *e2510* embryos arrested between 1-fold and 1.5-fold, while many of the *e2501* and *w37* embryos reached the pretzel stage and some even hatched, eventually dying as L1 larvae (Table 1). Even for the nearly fully elongated embryos, the elongation process was significantly slower than normal (Fig. 4A, data not shown). For example, *e2501* embryos did not reach the 3-fold stage until 10 hours, in contrast to the 8.5 hours for wild-type embryos.

Among the three alleles, *e2510* showed the severest defects in both accumulation of excess corpses and body elongation. *e2510* appeared to be neither a hypomorph nor an amorph, but to be a neomorph that possessed a function that was detrimental to embryogenesis only when two copies are present: *Df/e2510* embryos showed similar defects in cell death and elongation to those of the *w37* embryos (Fig. 2D-E; Table 1).

In wild-type embryos, the pharyngeal precursors surrounded by the basement membrane move anteriorly toward the buccal opening and connect to it during the comma to 1.5-fold stage (Fig. 4A) (Portereiko and Mango, 2001). The pharynx elongates further as the body extends longitudinally (Fig. 4A). In all *cdl-1* homozygous mutants, the pharyngeal basement membrane was almost always visible, but the pharynx was never connected with the buccal opening (Fig. 1). However, other morphological features of pharynx, including the grinder, looked normal, and muscular contraction of the pharynx (pumping) was often observed. Immunofluorescence microscopy with pharynx-specific antibody 3NB12 (Priess and Thomson, 1987) confirmed that the pharynx underwent at least early differentiation in *cdl-1* embryos (Fig. 4B,C).

Pharyngeal detachment seen in *cdl-1* embryos might be the result of a failure in the movement of the pharyngeal primordium toward the buccal opening. Alternatively, the pharynx might initially connect with, and later disjoint from, the anterior of the head. To distinguish these possibilities, we observed the development of the pharynx by 4D video microscopy. We found that the pharynx primordium did not move anteriorly throughout embryogenesis in *cdl-1* embryos (Fig. 4A). This defect in pharynx extension was seen in *cdl-1* embryos that elongated to over 3-fold as well as ones arrested at the 1- to 1.5-fold stage. Thus, the pharyngeal elongation defect is not a consequence of the body elongation defect. Rather, the function of *cdl-1* appears to be essential for the movement of pharyngeal cells toward the buccal opening.

To examine whether the lethality and the morphological defects of *cdl-1* embryos are the results of abnormal cell deaths, we observed morphogenesis of *cdl-1(e2510); ced-3(n717)*, *cdl-1(e2510); ced-4(n1162)* and *cdl-1(e2510); ced-9(n1950gf)* double mutant embryos (Ellis et al., 1991;

Table 1. Body elongation defect in *cdl-1* embryos

	Terminal elongation (%)					
Genotype	Before elongation	Lima bean	1.5-fold	2-fold	pretzel†	*n*
e2510	29	30	21	13	6	150
e2501	5	10	8	27	52	62
w37	5	3	13	13	67	64
*Df/e2510**	3	0	3	3	91	35
e2510; ced-3	28	28	16	21	7	35

Embryos collected from *cdl-1* heterozygous adults were grown at 20°C overnight. Dead embryos exhibiting the typical pharyngeal defect were scored for elongation.

**Df/e2510* embryos were generated by crossing *Df/+* heterozygous hermaphrodites with *e2510/+* heterozygous males.

†Embryos elongated over 3-fold.

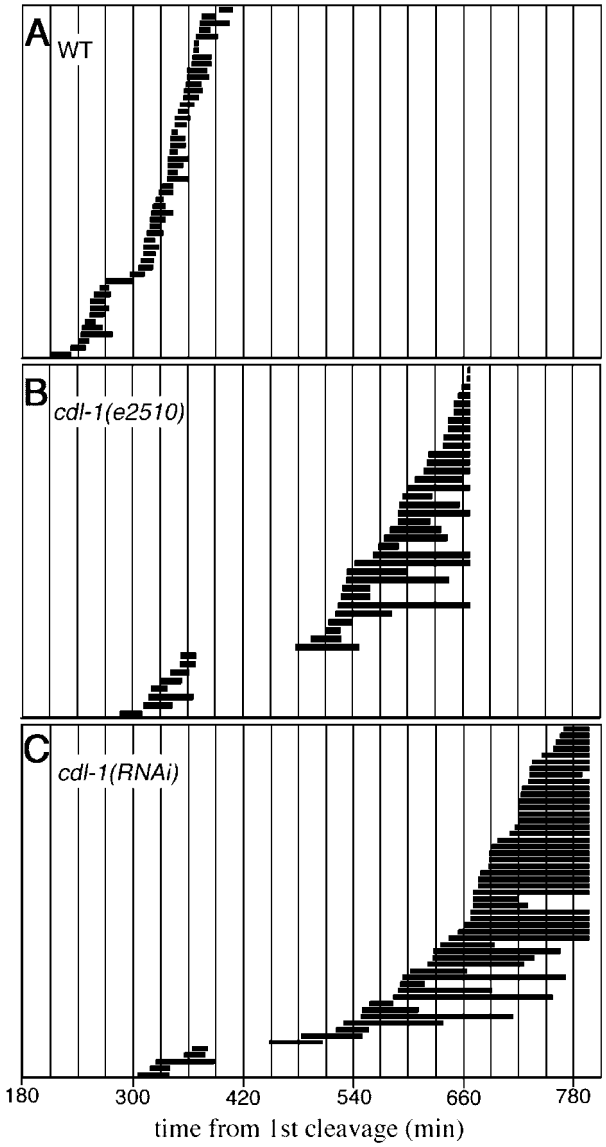

Fig. 3. Duration of visible cell corpses. (A) Wild-type N2. (B) *cdl-1(e2510)*. (C) *cdl-1(RNAi)*. Each panel illustrates the time of appearance and disappearance of all corpses detected in 4D images of a single embryo. (A typical result is displayed here for each genotype.) Each horizontal bar represents a corpse, and its length indicates duration of the corpse. The corpses are ordered according to the time of their appearance in the embryo. Scoring of corpses in N2 (A) was discontinued at ~400 minutes, because the twitching movement made observation of corpses difficult. For B and C, cell corpses were scored until the end of the time-lapse recording at 668 minutes (B) and 797 minutes (C) after first cleavage, respectively.

Hengartner et al., 1992), in which production of cell corpses was blocked as described above. Neither the lethality nor the elongation defect was suppressed in these double mutants (Table 1, data not shown). We confirmed by 4D microscopy and immunostaining of the pharynx that the pharyngeal phenotype of *cdl-1(e2510)* is unaffected by a *ced-3* mutation (data not shown). Thus, we conclude that the lethality and morphological defects of *cdl-1* embryos are not caused by aberrant cell death.

cdl-1 encodes a homologue of stem-loop binding proteins

The *cdl-1* gene encodes a 367 amino acid protein that shows significant similarity to the stem-loop binding proteins (SLBPs) in the RNA binding domain (Fig. 5A) (Wang et al., 1996). CDL-1 and mouse SLBP share 71% identity in this domain (Fig. 5B). We identified the molecular lesion in each of the three *cdl-1* alleles. Consistent with the results of genetic analysis (Fig. 2; Table 1), *w37* turned out to be a null allele that deletes the entire ORF of *cdl-1* (Fig. 5C). In contrast, *e2510* carried a missense mutation switching an evolutionarily conserved proline to serine at the 249th amino acid, and *e2501* carried a nonsense mutation at the 260th amino acid causing truncation of the carboxyl end of the RNA binding domain (Fig. 5B).

SLBPs bind specifically to the stem-loop structure in the 3′-UTR of replication-dependent histone mRNAs (Martin et al., 1997; Sullivan et al., 2001; Wang et al., 1996). Unlike other metazoan mRNAs, mature mRNAs of the replication-dependent histones are not polyadenylated, but instead contain a conserved stem-loop structure at the 3′ termini (Osley, 1991). SLBPs are implicated in histone pre-mRNA processing and translation of mature histone mRNA through tight association with the stem-loop structure (Dominski et al., 1995; Dominski et al., 1999; Martin et al., 1997; Muller et al., 2000; Sullivan et al., 2001; Wang et al., 1996).

It has been reported for *C. elegans* that some core histone genes share a common flanking sequence element; a conserved sequence of 34 bases that may form a stem-loop structure is present in the 3′-UTR of the genes (Roberts et al., 1989). We searched the *C. elegans* genome sequence (*C. elegans* Sequencing Consortium, 1998) for this conserved 34 bp sequence, and have found that 64 out of 71 core histone genes contain the sequence at their 3′ end with only minor divergence. Most of these core histone genes consist of a single exon, characteristic of replication-dependent histone genes in various organisms (Osley, 1991). Thus, we supposed it to be plausible that CDL-1 regulates stem-loop-carrying core histone mRNAs.

CDL-1 protein binds to the stem-loop structure in the 3′-UTR of *C. elegans* core histone mRNA

We used the yeast three-hybrid system to examine whether CDL-1 has the ability to bind to the conserved stem-loop forming sequence in the core histone mRNAs (Fig. 6A) (Martin et al., 1997; SenGupta et al., 1996; Wang et al., 1996). We connected the 34-nucleotide sequence conserved in *C. elegans* histone mRNA stem-loops to the 3′ end of the bait RNA (wtRNA) (Fig. 6B) (Roberts et al., 1989). To confirm the binding specificity, we also constructed a mutant bait RNA containing the same 34-nucleotide sequence except that the stem-loop structure was reversed (rvRNA) (Fig. 6B) (Wang et al., 1996). We found that full length CDL-1 fused with the GAL4 activation domain effectively binds to wtRNA, but not to rvRNA (Fig. 6C,D). These results indicate that CDL-1 interacts specifically with the stem-loop sequence in the 3′-UTR of *C. elegans* core histone mRNA confirming the results of Michel et al. (2000).

Since both *cdl-1(e2510)* and *cdl-1(e2501)* carried mutations in the RNA binding domain (Wang et al., 1996), the ability of these mutant proteins to bind to the stem-loop was also

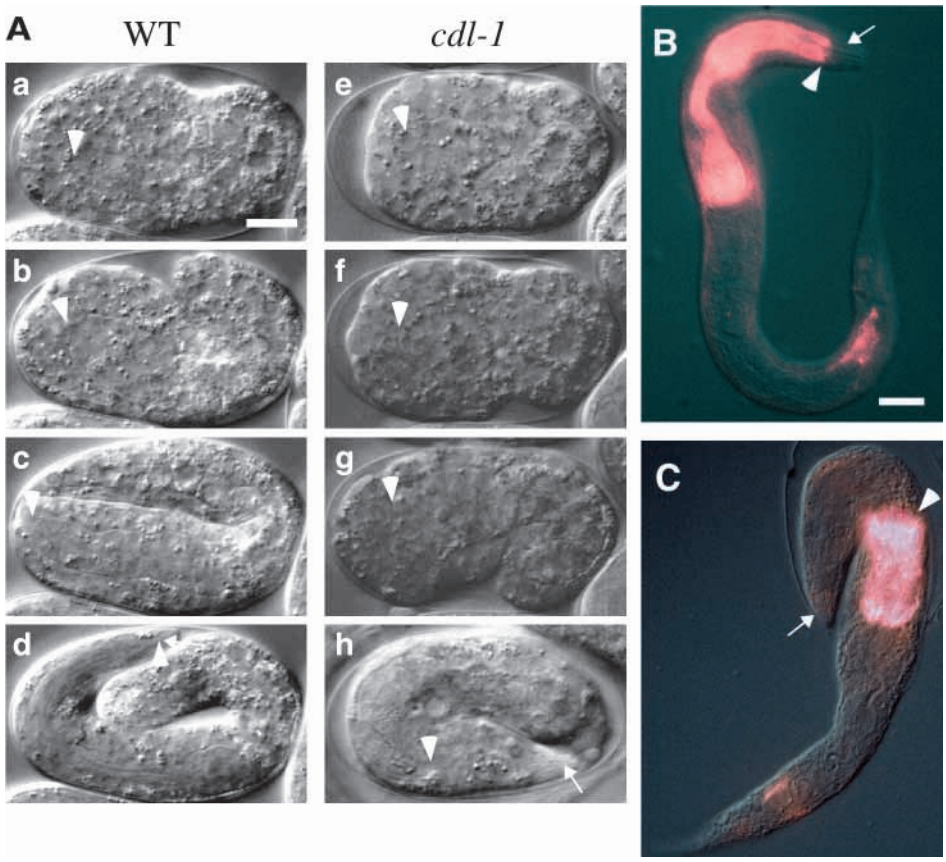

Fig. 4. Defects in pharynx morphogenesis in *cdl-1* mutant embryos. (A) Movement of the pharynx primordium toward the anterior of the head. Each picture was taken from a 4D recording of the same embryo. (a-d) Wild type and (e-h) *cdl-1(e2501)*. Arrowheads indicate the anterior tips of the pharyngeal basement membrane. The buccal capsule is indicated in d and h (arrows). Time from first cleavage: (a) 390 minutes, (b) 435 minutes, (c) 480 minutes, (d) 610 minutes, (e) 390 minutes, (f) 480 minutes, (g) 600 minutes, and (h) 1140 minutes. (B, C) Merged images of immunostaining with a pharynx-specific antibody, 3NB12 (red), and Nomarski microscopy. A wild-type N2 L1 larva (B) and a *cdl-1(e2501)* embryo (C) that has elongated over 3-fold are shown. The buccal capsule (arrow) and the anterior tip of the pharynx (arrowhead) are indicated.

examined. The CDL-1(P249S) protein, which corresponds to the protein product of *cdl-1(e2510)*, did not show interaction with either of the stem-loops. However, CDL-1(W260stop), which corresponds to the protein product of *cdl-1(e2501)*, showed weak interaction with both wtRNA and rvRNA (Fig. 6C,D). These results suggest that CDL-1 functions through its RNA binding ability, and that CDL-1 and core histone mRNA can form a complex in vivo. Therefore, it is likely that *cdl-1* regulates core histone expression, as suggested for SLBPs in other organisms.

Chromosome condensation during mitosis fails in *cdl-1(RNAi)* embryos

We performed RNA interference (RNAi) (Fire et al., 1998) for *cdl-1*. Although some F_1 embryos phenocopied the *cdl-1* genomic mutants (see Materials and Methods), the predominant phenotype of *cdl-1(RNAi)* was embryonic arrest at ~50 cells (Fig. 7A). To clarify the defect in these early arresting embryos, we examined the early mitotic cycles (Fig. 8). In wild-type animals, chromosomes are highly condensed from metaphase through telophase (Fig. 8A,B). Strikingly, *cdl-1(RNAi)* embryos that arrested early in embryogenesis failed to undergo proper condensation of chromosomes during the cell cycle, as evidenced by appearance of decondensed chromosomes from metaphase through telophase and interconnecting chromosome bridges (Fig. 8C,D). In addition, chromatin fragments were often observed outside the nucleus (data not shown). Thus, we conclude that abnormal

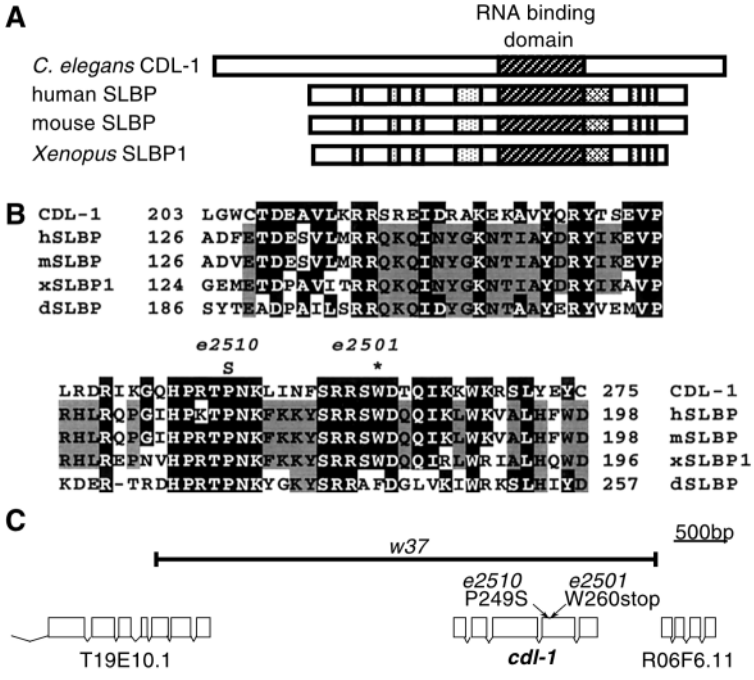

Fig. 5. The *cdl-1* gene. (A) Domain structures of CDL-1 and related proteins. The RNA stem-loop binding domain (striped boxes) are shared by all four proteins. Other domains conserved in the vertebrate proteins are not found in CDL-1. (B) Sequence alignment of the RNA binding domain of CDL-1 with human (hSLBP), mouse (mSLBP), *Xenopus* (xSLBP1) and *Drosophila* (dSLBP) SLBPs. The mutated residues in *e2510* (P-to-S missense mutation) and *e2501* (nonsense mutation) are indicated. (C) Structure of the *cdl-1* ORF. The mutation sites in *e2510* and *e2501* and the deleted region in *w37* are indicated. The neighboring predicted ORFs are also shown.

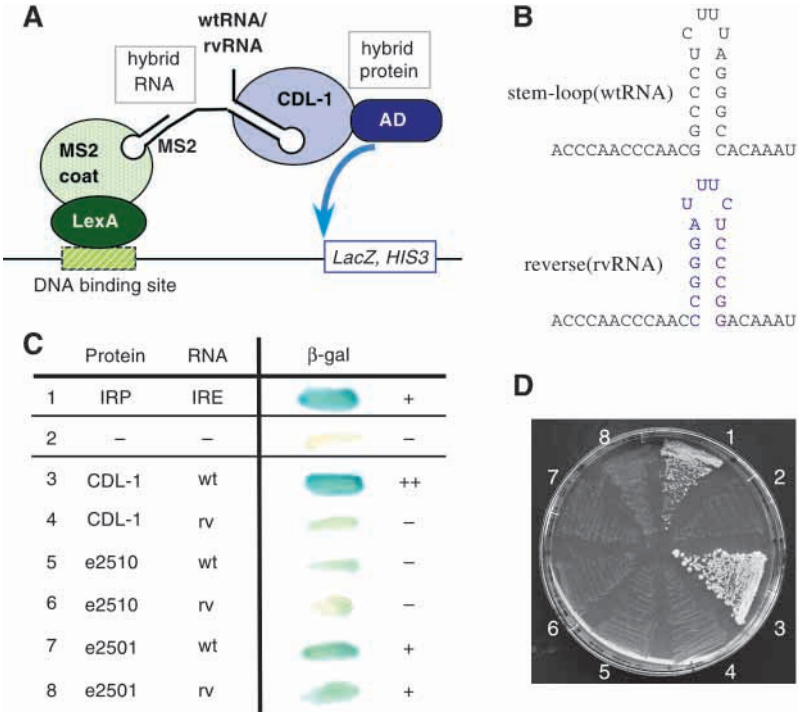

Fig. 6. CDL-1 interacts with the stem-loop structure in the 3′-UTR of core-histone mRNA. (A) The yeast three-hybrid system (SenGupta et al., 1996) was used to test the RNA binding specificity of CDL-1. The assay is schematically shown. (B) Structure of the two stem-loop RNAs used in the experiments. wtRNA: the conserved stem-loop sequence in the 3′-UTR of *C. elegans* core histone mRNA. rvRNA: the sequence with a reversed stem-loop. (C) RNA-binding activity of CDL-1 protein as assayed by β-galactosidase activity. IRE (Iron Response Element) and IRP (Iron Response Protein) were used as a pair of positive controls (SenGupta et al., 1996). (D) Activation of *HIS3*. Transformants indicated in C were streaked on –His plates containing 5 mM 3-aminotriazol.

chromosome condensation and segregation may be the major cause for the early arrest of the *cdl-1(RNAi)* embryos.

RNAi of histone genes mimics the phenotypes of *cdl-1* mutants

To examine whether the *cdl-1* phenotypes are the result of a shortage of core histone proteins, we performed RNAi to interfere with expression of each of the core histones H2A, H2B, H3 and H4. Because each of the histone gene family is highly conserved, RNAi of one member of a class can be expected to inhibit expression of all members of the same class (Parrish et al., 2000). The resulting RNAi embryos for any of the four gene classes showed an early arrest phenotype similar to that of the *cdl-1(RNAi)* embryos (Fig. 7D). DAPI staining revealed that embryos affected by RNAi of the histone genes often exhibited decondensed chromosomes from metaphase through telophase, and chromosome bridges, as seen in the *cdl-1(RNAi)* embryos (Fig. 8E,F).

From these observations, we presume that production of histone protein is decreased in *cdl-1(RNAi)* embryos, further supporting the possibility that *cdl-1* regulates the expression of core histones at the post-transcriptional level in vivo.

To examine whether the zygotic phenotypes of *cdl-1* mutants are also the result of decreased histone gene expression, we observed the late embryonic phenotypes of RNAi of histone genes. Some embryos that were subjected to RNAi of the gene class for either of histone H2A, H2B, H3 or H4 phenocopied the zygotic chromosomal *cdl-1* mutants (Fig. 7B,C,E,F). Such embryos contained excess cell corpses (up to 15 corpses/embryo), had defects

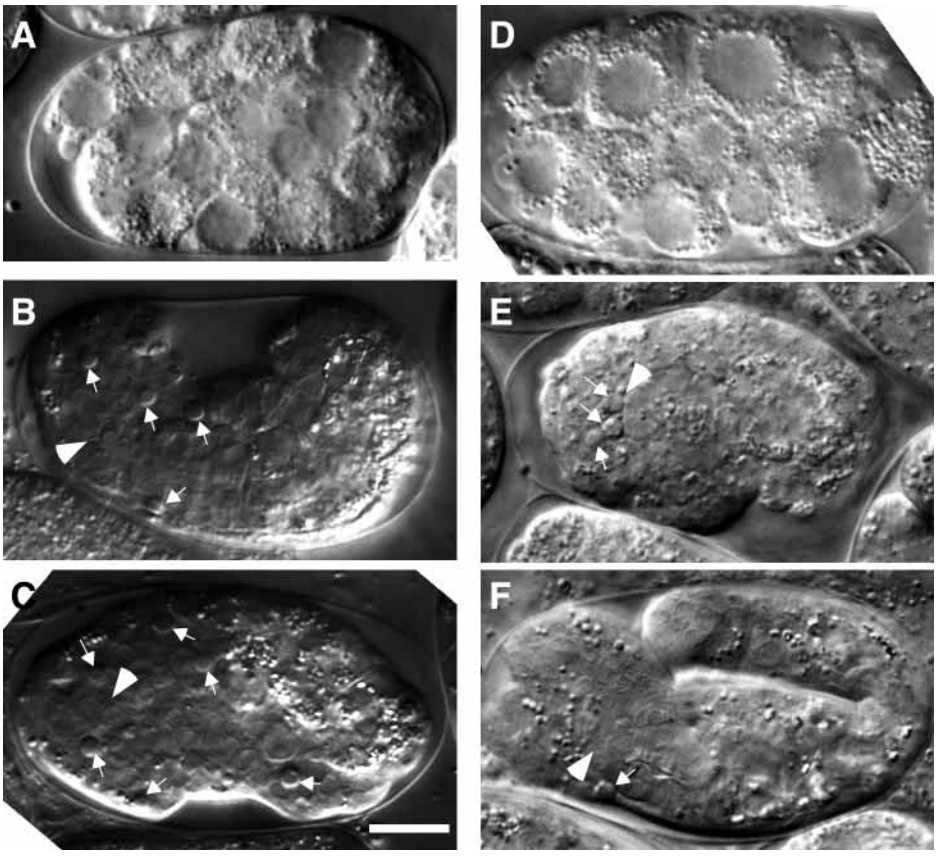

Fig. 7. RNAi phenotypes of *cdl-1* and core histone genes. (A,D) The predominant RNAi phenotypes for *cdl-1* (A) and the histone H4 gene (D). Embryos arrest with around 50 cells in both cases. (B,C,E,F) Embryos showing later embryonic RNAi phenotypes, which are similar to those of the *cdl-1* mutants. (B,C) *cdl-1*, (E,F) the histone H2B gene. Arrows indicate cell corpses. Arrowheads indicate the anterior tip of the pharynx. Scale bar, 10 μm.

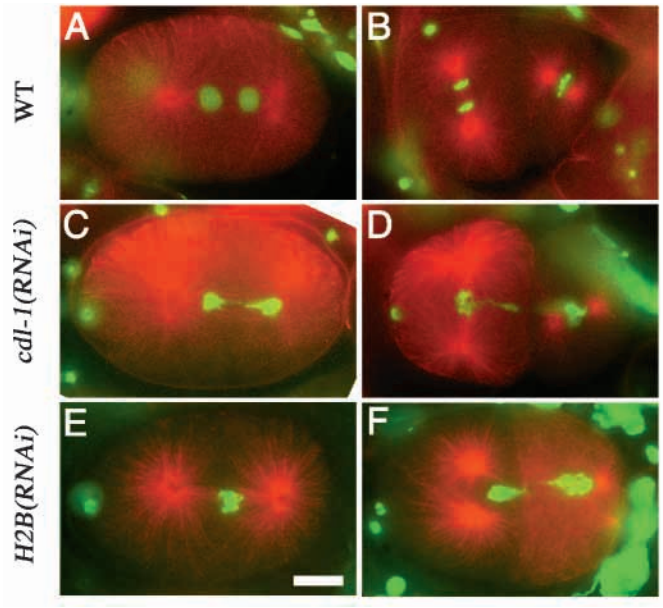

Fig. 8. RNAi of either *cdl-1* or the histone genes resuls in defects in chromosome condensation and segregation. Embryos co-stained with the anti-alpha tubulin antibody (red) and DAPI (green) are shown. (A,B) Wild type. (C,D) *cdl-1(RNAi)*. (E,F) RNAi of the histone H2B gene. In wild type, chromosomes are properly condensed at metaphase (B right) and segregated at anaphase (B left) through telophase (A). In embryos in which CDL-1 or histones are depleted, chromosome bridges (C,D,F) and decondensed chromosomes at metaphase and anaphase (D,E) can be often observed. Scale bar, 10 μm.

in body elongation, and detached pharynxes at the terminal stage. A delay in appearance and elimination of cell corpses were also seen in these embryos (data not shown). Thus, we conclude that *cdl-1* regulates core histone gene expression not only in early cell division but also in late embryogenesis.

DISCUSSION

The role of *cdl-1* in core histone expression

CDL-1 was previously identified by others as a homolog of mammalian SLBP/HBPs and characterized biochemically (Michel et al., 2000). It was shown that CDL-1 possesses specific binding activity to the stem-loop structure of *C. elegans* histone mRNAs. Our finding that reduction of *cdl-1* function and that of the function of any core histone cause indistinguishable phenotypes (Fig. 7, Fig. 8) strongly suggests that CDL-1 is indeed essential for proper histone expression in *C. elegans* development.

We found that the conserved 34 bp stem-loop sequence is present in the core histone mRNAs (Roberts et al., 1989). There are 64 stem-loop sequences identifiable in the *C. elegans* genome, all of which reside downstream of the core histone ORFs. We have also found seven putative core histone genes in the genome that do not carry the stem-loop sequence. Thus, the majority (64/71) of core histone genes in *C. elegans* contain the stem-loop sequence. Considering the stringent binding specificity of CDL-1 (Michel et al., 2000), we speculate that the core histone mRNAs are the only targets of CDL-1. In addition, unlike *Xenopus laevis*, which expresses at least two SLBPs (xSLBP1 and xSLBP2) (Wang et al., 1999), *C. elegans* has no other SLBP-like protein. Thus, CDL-1 is likely to be responsible for post-transcriptional regulation of the majority of the core histone genes in *C. elegans*.

Drosophila melanogaster is the only other organism in which the function of SLBP has been genetically examined (Sullivan et al., 2001). dSLBP, the *Drosophila* SLBP, is both zygotically and maternally required, and loss-of-function mutant embryos exhibit similar defects in chromosome condensation and segregation, as those we have observed in *cdl-1(RNAi)* embryos.

Molecular nature of the *cdl-1* mutations

The three alleles of *cdl-1* turned out to be distinct types of mutations. *w37* is an apparent null allele (Fig. 5C). The other two alleles have mutations in the RNA binding domain, which is conserved among the SLBP/HBPs (Fig. 5B). Interestingly, the null allele *w37* exhibited milder defects in both cell corpse accumulation and body elongation than the two other alleles, which appear to produce mutant proteins with reduced RNA-binding ability (Fig. 2; Table 1). How do the mutant forms of CDL-1 cause severer phenotypes than the null allele? One possibility might be that the mutant forms titrate out factors involved in histone mRNA processing. A proposed function for SLBP in vertebrate is to facilitate the interaction between U7 snRNP and histone pre-mRNA (Dominski et al., 1999). U7 snRNP plays an essential role in the processing reaction, associating with pre-mRNAs through base-pairing. SLBP is not required for cleavage of the 3′ sequence of pre-mRNAs if U7 snRNP can stably interact with them (Streit et al., 1993). In vertebrates, other factors than U7 snRNP, including the heat labile factor (HLF) (Gick et al., 1987) and a hypothetical cleavage factor (CF) (Dominski and Marzluff, 1999), have been also suggested to participate in the 3′ processing of histone mRNAs. Although these factors have not been identified in *C. elegans*, it is possible that titration of any of these factors by the mutant CDL-1 proteins results in further reduction of the processing activity than occurs in the absence of CDL-1 protein. Alternatively, an altered RNA-binding specificity of the mutant proteins might interfere with expression of some other mRNAs, which results in additional defects in development.

The role of *cdl-1* in programmed cell death

Cells undergoing programmed cell death in *C. elegans* show morphological and biochemical changes similar to mammalian apoptotic cells. A cell that dies by programmed cell death in *C. elegans* appears as a highly refractile disk (Sulston and Horvitz, 1977). This morphological change probably corresponds to the pycnosis of the dying cell, in which the chromatin aggregates and DNA is degraded (Robertson and Thomson, 1982). Although genes that participate in the initiation of killing have been well characterized in *C. elegans* (reviewed by Metzstein et al., 1998), it remains unclear how the dying cells undergo the ensuing morphological changes associated with apoptosis.

The appearance of cell corpses is delayed, and the corpses persisted much longer in *cdl-1* mutant embryos than in the wild type (Fig. 3). These phenotypes imply that the progression of the cell death program is slowed down in *cdl-1* mutants. *ced-*

8 is the only other gene known to affect the kinetics of programmed cell death (Stanfield and Horvitz, 2000). In *ced-8* mutants, embryonic programmed cell death proceeds slowly; however, unlike in *cdl-1* mutants, the engulfment process is not affected and proceeds at a normal rate. Therefore, *cdl-1* and *ced-8* are likely to function in distinct processes in programmed cell death.

Why does a defect in *cdl-1* activity result in the cell death phenotypes? Chromatin condensation during apoptosis in mammals involves a stereotypical structural change at the nucleosomal level. There are several reports demonstrating that core histone modifications occur during apoptosis and that such modifications affect chromatin condensation in dying cell nuclei (reviewed by Robertson et al., 2000). For example, deacetylation of histone H4 (Allera et al., 1997), phosphorylation of H2B (Ajiro, 2000), and phosphorylation of H2A.X (an H2A variant) (Rogakou et al., 2000) have been observed during apoptosis. Thus, it is plausible that a limiting amount of histones in the *cdl-1* mutants blocks formation of the chromatin structure required for proper progression of cell death. Alternatively, an alteration in the expression levels of various genes caused by aberrant chromatin structure (see below) may interfere with the cell death process.

The role of *cdl-1* in morphogenesis

All *cdl-1* mutants exhibited highly penetrant specific defects in pharynx development and body elongation (Table 1; Fig. 4), though the extent of body elongation varied (Table 1). These cell-type specific defects were rather surprising, considering that *cdl-1* is involved in histone expression, which would be expected to affect every cell. Since these morphogenetic events occur after the cell proliferation stage, and are dependent on cell shape change, the observed phenotypes are unlikely to be the results of cell cycle defects. Rather, these morphogenetic phenotypes may be attributable to misexpression of certain genes as the result of disturbed chromatin structure.

Transcriptional activity is regulated in part through chromatin modifications. For example, histone hyperacetylation/hypoacetylation contributes to transcriptional activation/repression (reviewed by Cheung et al., 2000). Furthermore, in vivo studies have demonstrated the involvement of histone acetylation and deacetylation multiprotein complexes in development (reviewed by Ahringer, 2000; Cheung et al., 2000). For example, the *C. elegans egl-27* and *egr-1* genes, which encode components of a major histone deacetylase complex, NuRD (nucleosome remodeling and histone deacetylation), were shown to be required for the expression of the *hlh-8* gene and for proper organization of various tissues, including the pharynx (Solari et al., 1999). The *C. elegans* histone acetylation (HAT) complex is involved in signaling pathways important for pattern formation (Shi and Mello, 1998). In addition, chromatin-remodeling complexes such as SWI/SNF change the local transcription activity by altering nucleosome structure (reviewed by Peterson and Workman, 2000). Because mutations in *cdl-1* would be expected to cause a shortage of core histone proteins, which might lead to disturbed chromatin structure, it is conceivable that regulation of gene expression by histone acetylation/deacetylation or chromatin-remodeling might be severely affected accordingly. The resulting misexpression of various genes might lead to tissue- or cell-type-specific developmental defects. We speculate that hypodermal and pharyngeal cells may be more susceptible to disturbance in chromatin structure than others, thereby causing the specific morphological defects seen in these mutants.

We thank S. Mango for critical reading of the manuscript, and M. Ohmachi, E. Lambie, P. Kuwabara and T. Schedl for sharing unpublished results. We are grateful to the following people for providing materials used in this work: Y. Kohara for cDNA clones, M. Wickens for materials used in the yeast three-hybrid system, C. Thomas for the 4D recording software, and M. Koga for pPDEF1α. Some of the strains used in this work were provided by the Caenorhabditis Genetics Center, which is funded by the National Center for Research Resources of the National Institutes of Health. The cosmid transgenic strain was provided by the *C. elegans* Transgenic Library Project, funded by a grant to A. Rose and D. Baillie from the Canadian Genome Analysis and Technology Program (CGAT). J. H. R. is grateful to J. White for providing laboratory space and supplies during the initial phases of this work. This work was supported by grants from the Japan Science and Technology Corporation (A. S.), a Grant-in-Aid for Specially Promoted Research from the Ministry of Education, Culture, Sports, Science and Technology of Japan (M. Y.), and a Helen Hay Whitney Postdoctoral Fellowship, a Chicago Community Trust/Searle Scholars Award, a Milwaukee Foundation/Shaw Scientists Award, and grants from the National Institutes of Health and the March of Dimes (J. H. R.). Y. K. was supported by a Research Fellowship (DC) from the Japan Society for the Promotion of Science (JSPS).

REFERENCES

Ahringer, J. (2000). NuRD and SIN3 histone deacetylase complexes in development. *Trends Genet.* **16**, 351-356.

Ajiro, K. (2000). Histone H2B phosphorylation in mammalian apoptotic cells. An association with DNA fragmentation. *J. Biol. Chem.* **275**, 439-443.

Allera, C., Lazzarini, G., Patrone, E., Alberti, I., Barboro, P., Sanna, P., Melchiori, A., Parodi, S. and Balbi, C. (1997). The condensation of chromatin in apoptotic thymocytes shows a specific structural change. *J. Biol. Chem.* **272**, 10817-10822.

Brenner, S. (1974). The genetics of *Caenorhabditis elegans*. *Genetics* **77**, 71-94.

***C. elegans* Sequencing Consortium.** (1998). Genome sequence of the nematode *C. elegans*: a platform for investigating biology. The *C. elegans* Sequencing Consortium. *Science* **282**, 2012-2018.

Cheung, P., Allis, C. D. and Sassone-Corsi, P. (2000). Signaling to chromatin through histone modifications. *Cell* **103**, 263-271.

Dominski, Z. and Marzluff, W. F. (1999). Formation of the 3′ end of histone mRNA. *Gene* **239**, 1-14.

Dominski, Z., Sumerel, J., Hanson, R. J. and Marzluff, W. F. (1995). The polyribosomal protein bound to the 3′ end of histone mRNA can function in histone pre-mRNA processing. *RNA* **1**, 915-923.

Dominski, Z., Zheng, L. X., Sanchez, R. and Marzluff, W. F. (1999). Stem-loop binding protein facilitates 3′-end formation by stabilizing U7 snRNP binding to histone pre-mRNA. *Mol. Cell. Biol.* **19**, 3561-3570.

Ellis, H. M. and Horvitz, H. R. (1986). Genetic control of programmed cell death in the nematode *C. elegans*. *Cell* **44**, 817-829.

Ellis, R. E., Jacobson, D. M. and Horvitz, H. R. (1991). Genes required for the engulfment of cell corpses during programmed cell death in *Caenorhabditis elegans*. *Genetics* **129**, 79-94.

Fire, A., Xu, S., Montgomery, M. K., Kostas, S. A., Driver, S. E. and Mello, C. C. (1998). Potent and specific genetic interference by double-stranded RNA in *Caenorhabditis elegans*. *Nature* **391**, 806-811.

Gallie, D. R., Lewis, N. J. and Marzluff, W. F. (1996). The histone 3′-terminal stem-loop is necessary for translation in Chinese hamster ovary cells. *Nucleic Acids Res.* **24**, 1954-1962.

Gick, O., Kramer, A., Vasserot, A. and Birnstiel, M. L. (1987). Heat-labile regulatory factor is required for 3′ processing of histone precursor mRNAs. *Proc. Natl. Acad. Sci. USA* **84**, 8937-8940.

Harris, M. E., Bohni, R., Schneiderman, M. H., Ramamurthy, L.,

Schumperli, D. and Marzluff, W. F. (1991). Regulation of histone mRNA in the unperturbed cell cycle: evidence suggesting control at two posttranscriptional steps. *Mol. Cell Biol.* **11**, 2416-2424.

Hengartner, M. O., Ellis, R. E. and Horvitz, H. R. (1992). *Caenorhabditis elegans* gene *ced-9* protects cells from programmed cell death. *Nature* **356**, 494-499.

Ingledue, T. C., III, Dominski, Z., Sanchez, R., Erkmann, J. A. and Marzluff, W. F. (2000). Dual role for the RNA-binding domain of *Xenopus laevis* SLBP1 in histone pre-mRNA processing. *RNA* **6**, 1635-1648.

Janke, D. L., Schein, J. E., Ha, T., Franz, N. W., O'Neil, N. J., Vatcher, G. P., Stewart, H. I., Kuervers, L. M., Baillie, D. L. and Rose, A. M. (1997). Interpreting a sequenced genome: toward a cosmid transgenic library of *Caenorhabditis elegans*. *Genome Res.* **7**, 974-985.

Kornberg, R. D. and Lorch, Y. (1999). Twenty-five years of the nucleosome, fundamental particle of the eukaryote chromosome. *Cell* **98**, 285-294.

Luscher, B. and Schumperli, D. (1987). RNA 3′ processing regulates histone mRNA levels in a mammalian cell cycle mutant. A processing factor becomes limiting in G1-arrested cells. *EMBO J.* **6**, 1721-1726.

Ma, T., Van Tine, B. A., Wei, Y., Garrett, M. D., Nelson, D., Adams, P. D., Wang, J., Qin, J., Chow, L. T. and Harper, J. W. (2000). Cell cycle-regulated phosphorylation of p220(NPAT) by cyclin E/Cdk2 in Cajal bodies promotes histone gene transcription. *Genes Dev.* **14**, 2298-2313.

Martin, F., Schaller, A., Eglite, S., Schumperli, D. and Muller, B. (1997). The gene for histone RNA hairpin binding protein is located on human chromosome 4 and encodes a novel type of RNA binding protein. *EMBO J.* **16**, 769-778.

Mello, C. and Fire, A. (1995). DNA transformation. *Methods Cell. Biol.* **48**, 451-482.

Mello, C. C., Kramer, J. M., Stinchcomb, D. and Ambros, V. (1991). Efficient gene transfer in *C. elegans*: extrachromosomal maintenance and integration of transforming sequences. *EMBO J.* **10**, 3959-3970.

Metzstein, M. M., Stanfield, G. M. and Horvitz, H. R. (1998). Genetics of programmed cell death in *C. elegans*: past, present and future. *Trends Genet.* **14**, 410-416.

Michel, F., Schumperli, D. and Muller, B. (2000). Specificities of *Caenorhabditis elegans* and human hairpin binding proteins for the first nucleotide in the histone mRNA hairpin loop. *RNA* **6**, 1539-1550.

Miller, D. M. and Shakes, D. C. (1995). Immunofluorescence microscopy. *Methods Cell Biol.* **48**, 365-394.

Mowry, K. L., Oh, R. and Steitz, J. A. (1989). Each of the conserved sequence elements flanking the cleavage site of mammalian histone pre-mRNAs has a distinct role in the 3′-end processing reaction. *Mol. Cell. Biol.* **9**, 3105-3108.

Muller, B., Link, J. and Smythe, C. (2000). Assembly of U7 small nuclear ribonucleoprotein particle and histone RNA 3′ processing in *Xenopus* egg extracts. *J. Biol. Chem.* **275**, 24284-24293.

Muller, B. and Schumperli, D. (1997). The U7 snRNP and the hairpin binding protein: Key players in histone mRNA metabolism. *Semin. Cell Dev. Biol.* **8**, 567-576.

Osley, M. A. (1991). The regulation of histone synthesis in the cell cycle. *Annu. Rev. Biochem.* **60**, 827-861.

Pandey, N. B. and Marzluff, W. F. (1987). The stem-loop structure at the 3′ end of histone mRNA is necessary and sufficient for regulation of histone mRNA stability. *Mol. Cell Biol.* **7**, 4557-4559.

Parrish, S., Fleenor, J., Xu, S., Mello, C. and Fire, A. (2000). Functional anatomy of a dsRNA trigger. Differential requirement for the two trigger strands in RNA interference. *Mol. Cell* **6**, 1077-1087.

Peterson, C. L. and Workman, J. L. (2000). Promoter targeting and chromatin remodeling by the SWI/SNF complex. *Curr. Opin. Genet. Dev.* **10**, 187-192.

Portereiko, M. F. and Mango, S. E. (2001). Early Morphogenesis of the *Caenorhabditis elegans* Pharynx. *Dev. Biol.* **233**, 482-494.

Priess, J. R. and Hirsh, D. I. (1986). *Caenorhabditis elegans* morphogenesis: the role of the cytoskeleton in elongation of the embryo. *Dev. Biol.* **117**, 156-173.

Priess, J. R. and Thomson, J. N. (1987). Cellular interactions in early *C. elegans* embryos. *Cell* **48**, 241-250.

Roberts, S. B., Emmons, S. W. and Childs, G. (1989). Nucleotide sequences of *Caenorhabditis elegans* core histone genes. Genes for different histone classes share common flanking sequence elements. *J. Mol. Biol.* **206**, 567-577.

Robertson, A. M. G. and Thomson, J. N. (1982). Morphology of programmed cell death in the ventral nerve cord of *Caenorhabiditis elegans* larvae. *J. Embryol. Exp. Morphol.* **67**, 89-100.

Robertson, J. D., Orrenius, S. and Zhivotovsky, B. (2000). Review: nuclear events in apoptosis. *J. Struct. Biol.* **129**, 346-358.

Rogakou, E. P., Nieves-Neira, W., Boon, C., Pommier, Y. and Bonner, W. M. (2000). Initiation of DNA fragmentation during apoptosis induces phosphorylation of H2AX histone at serine 139. *J. Biol. Chem.* **275**, 9390-9395.

SenGupta, D. J., Zhang, B., Kraemer, B., Pochart, P., Fields, S. and Wickens, M. (1996). A three-hybrid system to detect RNA-protein interactions in vivo. *Proc. Natl. Acad. Sci. USA* **93**, 8496-8501.

Shi, Y. and Mello, C. (1998). A CBP/p300 homolog specifies multiple differentiation pathways in *Caenorhabditis elegans*. *Genes Dev.* **12**, 943-955.

Solari, F., Bateman, A. and Ahringer, J. (1999). The *Caenorhabditis elegans* genes *egl-27* and *egr-1* are similar to MTA1, a member of a chromatin regulatory complex, and are redundantly required for embryonic patterning. *Development* **126**, 2483-2494.

Stanfield, G. M. and Horvitz, H. R. (2000). The *ced-8* gene controls the timing of programmed cell deaths in *C. elegans*. *Mol. Cell* **5**, 423-433.

Stauber, C., Luscher, B., Eckner, R., Lotscher, E. and Schumperli, D. (1986). A signal regulating mouse histone H4 mRNA levels in a mammalian cell cycle mutant and sequences controlling RNA 3′ processing are both contained within the same 80-bp fragment. *EMBO J.* **5**, 3297-3303.

Stauber, C. and Schumperli, D. (1988). 3′ processing of pre-mRNA plays a major role in proliferation-dependent regulation of histone gene expression. *Nucleic Acids Res.* **16**, 9399-9414.

Streit, A., Koning, T. W., Soldati, D., Melin, L. and Schumperli, D. (1993). Variable effects of the conserved RNA hairpin element upon 3′ end processing of histone pre-mRNA in vitro. *Nucleic Acids Res.* **21**, 1569-1575.

Sugimoto, A., Kusano, A., Hozak, R. R., Derry, W. B., Zhu, J. and Rothman, J. H. (2001). Many genomic regions are required for normal embryonic programmed cell death in *Caenorhabditis elegans*. *Genetics* **158**, 237-252.

Sullivan, E., Santiago, C., Parker, E. D., Dominski, Z., Yang, X., Lanzotti, D. J., Ingledue, T. C., Marzluff, W. F. and Duronio, R. J. (2001). *Drosophila* stem loop binding protein coordinates accumulation of mature histone mRNA with cell cycle progression. *Genes Dev.* **15**, 173-187.

Sulston, J. E. and Horvitz, H. R. (1977). Post-embryonic cell lineages of the nematode, *Caenorhabditis elegans*. *Dev. Biol.* **56**, 110-156.

Sulston, J. E., Schierenberg, E., White, J. G. and Thomson, J. N. (1983). The embryonic cell lineage of the nematode *Caenorhabditis elegans*. *Dev. Biol.* **100**, 64-119.

Sun, J., Pilch, D. R. and Marzluff, W. F. (1992). The histone mRNA 3′ end is required for localization of histone mRNA to polyribosomes. *Nucleic Acids Res.* **20**, 6057-6066.

Wang, Z. F., Ingledue, T. C., Dominski, Z., Sanchez, R. and Marzluff, W. F. (1999). Two *Xenopus* proteins that bind the 3′ end of histone mRNA: implications for translational control of histone synthesis during oogenesis. *Mol. Cell Biol.* **19**, 835-845.

Wang, Z. F., Whitfield, M. L., Ingledue, T. C., Dominski, Z. and Marzluff, W. F. (1996). The protein that binds the 3′ end of histone mRNA: a novel RNA-binding protein required for histone pre-mRNA processing. *Genes Dev.* **10**, 3028-3040.

Williams, A. S., Ingledue, T. C., 3rd, Kay, B. K. and Marzluff, W. F. (1994). Changes in the stem-loop at the 3′ terminus of histone mRNA affects its nucleocytoplasmic transport and cytoplasmic regulation. *Nucleic Acids Res.* **22**, 4660-4666.

Zhao, J., Kennedy, B. K., Lawrence, B. D., Barbie, D. A., Matera, A. G., Fletcher, J. A. and Harlow, E. (2000). NPAT links cyclin E-Cdk2 to the regulation of replication-dependent histone gene transcription. *Genes Dev.* **14**, 2283-2297.